Journal of
Nanoscience and Nanotechnology
Vol. 11, 10433–10437, 2011

Optimal Design of 3-D Carbon Microelectrode Array for Dielectrophoretic Manipulation of Nanoparticles in Fluids

Zirong Tang[1,*], Rizwan Malik[2], Jie Gong[1], Tielin Shi[2], and Shiyuan Liu[1]

[1] *Wuhan National Laboratory for Optoelectronics, Huazhong University of Science and Technology, Wuhan 430074, China*
[2] *State Key Laboratory of Digital Manufacturing Equipment and Technology, Huazhong University of Science and Technology, Wuhan 430074, China*

Manipulation of nanoparticles using nonuniform electric fields is an area of growing interest for nanotechnology applications. This article presents a design methodology and numerical analysis of electric fields and dielectrophoretic forces for 3-dimensional (3-D) carbon microelectrode array, overcoming the limitations of previous approaches. A description of the boundary element method is developed to compute electric field distribution much precisely. The effects of electrode shape, spacing, width and height on field distribution are considered. The results show that the gradient magnitude produced by square column electrodes is most effective to realize manipulation of nanoparticles in fluids. As both the electrode spacing and width are reduced the field gradient magnitude increases exponentially. By increasing the height of electrodes, the electric field extends largely in the electrode locality, which is advantageous to improve the manipulation efficiency with high degree of precision, flexibility and throughput. The theoretical predictions will provide design guides for 3-D carbon microelectrode array towards manipulation of nanoparticles in fluids, which have been shown in reasonable agreement with literature experimental reports.

Keywords: Manipulation, Dielectrophoresis, Carbon Microelectrode Array, Nanoparticles.

RESEARCH ARTICLE

1. INTRODUCTION

The manipulation of nanoparticles using electric fields has gained increasing importance with the development of miniaturized lab-on-a-chip type devices.[1–3] Dielectrophoresis (DEP) is a method exerting forces on particles via dipoles induced by electric field gradients.[4] The heart of these devices is mainly a set of microelectrodes producing a high gradient of electric field intensity that drives particles by DEP forces.[5] Depending on particle polarizability being higher or lower than that of the suspending medium, the force points out towards the high or low electric field regions and such phenomenon is called as positive or negative DEP respectively.

Previously, in the development of DEP technique, the key lies in constructing suitable configuration of electrodes to obtain proper nonuniform electric field for each specific sample.[6–9] However, most studies were based on inertial metal electrodes with 2-D planar structures, which are costly, not biocompatible and flexible. Meanwhile, most of the designs are plagued by a common problem of low throughput and efficiency since DEP force rapidly decays as the distance from the channel floor increases.[10] With the latest introduction of low-cost method of fabricating various 3-D glassy carbon MEMS (C-MEMS), novel applications with C-MEMS have been envisioned, especially in the field of DEP manipulation of nanoparticles within fluids.[11] By comparing with 2-D metallic electrodes, DEP manipulation devices with 3-D carbon microelectrode structures can largely extend the distribution of the electric field besides its better biocompatibility and broad electrochemical stability window.[12] However, conventional 2-D electrode design approach is not feasible for optimal design of 3-D microelectrodes. The effects of 3-D electrode configurations, including the possible on-chip integration for separation, transportation, trapping, sorting and detection, are numerous and still largely unexplored.

Computational simulations are one of essential steps in designing of appropriate electrodes and configurations for optimized device.[13] Both analytical and numerical approaches have previously been utilized to investigate field and DEP force distributions.[14–17] These studies generally assume some approximations such as simplified boundary conditions, linear variation of electric potential between adjacent electrodes, negligible influence of the

*Author to whom correspondence should be addressed.

medium conductivity and idealized electrodes with zero thickness. Here, we will accurately model the electric field distribution for various 3-D carbon electrode configurations through an improved description of the boundary element method based on Green's theorem. By comparative analysis, the shape of microelectrodes is determined first, then the effects of microelectrode width, spacing, height and the applied voltage on the spatial distribution of electric field and DEP forces are investigated and discussed for practical manipulations.

2. MODELING AND SIMULATION

Modeling of DEP for nano-scale spherical particles is often used to optimize the electrode geometry. As described by Pohl,[2] the first order or dipole contribution to the time-averaged DEP force for a spherical particle is given by $\langle \vec{F}_{\mathrm{DEP}} \rangle = 2\pi\varepsilon_m r^3 Re(f_{\mathrm{CM}})\nabla(\vec{E}\cdot\vec{E})$, where ε_m is the permittivity of the medium, r is the particle radius, $\mathrm{Re}(f_{\mathrm{CM}})$ is the real component of Clausius-Mossotti factor f_{CM}, and ∇ is the gradient operator of AC electric field E governed by the Maxwell equation. Because we are dealing with the electric field magnitude, AC electric field is regarded as electrostatic field. Space potential distribution satisfies Laplace equation $\nabla^2\Phi = 0$, where Φ is the potential in spatial position and the electric field distribution can be calculated by $\vec{E} = -\nabla\Phi$. We can obtain the numerical solution of the field potential through finite element software (Multiphysics COMSOL).

Considering that carbon microelectrode array is constructed to produce nonuniform field and arranged periodically, we select quadruple configuration of electrode array for modeling and simulation. The shapes of electrode are circular, square and triangular column respectively shown in Figure 1. The potential distribution of random point Φ satisfies Laplace's equation. An electric isolation condition of normal zero electric field $(\partial\Phi/\partial n = 0)$ is imposed to all boundaries other than electrode surface. The electrodes are assumed to be as ideal conductors, thus their surface potential is equal to the applied voltage V. In all cases, the projections of electrodes in X–Y plane are depicted

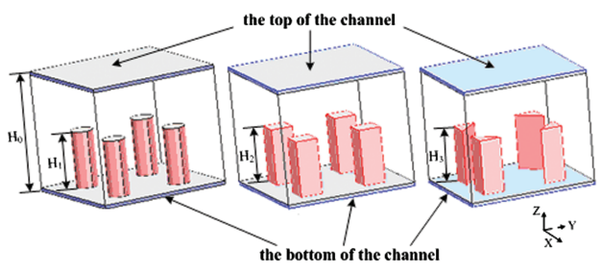

Fig. 1. Schematics of 3-D microelectrode array for nanoparticle manipulation in microchannel with extruded quadruple circular, square and triangular column configurations.

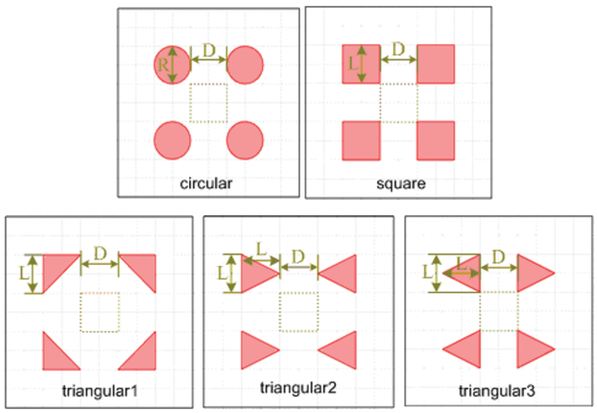

Fig. 2. Schematics of 3-D microelectrode array projection in X–Y plane.

in Figure 2, where three configurations of triangular column electrodes are designed and geometric parameters are displayed.

3. RESULTS AND DISCUSSION

Following simulation approach presented previously, some important results are obtained and critical discussions are also being illustrated below.

3.1. Dependence on Electrode Shape

As shown in Figure 3, the field gradient is plotted as a function of distance from channel floor for various electrode shapes. The electrode shapes are circular, square and three kinds of triangular column, respectively. It is observed that sharp edge electrodes (square, triangular2 and triangular3 in Fig. 2) produce the highest gradient magnitude of electric field, which is favorable to improve DEP force for nanoparticle manipulation such as particle separation, trapping, detection and etc. This prediction is also in agreement with literature experimental reports,[18] which demonstrated that sharp tip electrode structures (such as arrow head) are convenient to focus nanoparticle precisely towards the center of the channel at the large region with higher manipulation efficiency.[19] On the other hand, since square column electrode array with symmetrical configuration is also easily to be fabricated with C-MEMS process and its DEP device can be built easier, therefore square column electrode configuration is most suitable for DEP manipulation. The following investigations are all been done based on square shape of electrodes.

3.2. The Surface Plots of the Gradient in the Electric Field Intensity

Figure 4 depicts the surface plots of electric field intensity gradient produced by square column quadruple electrodes.

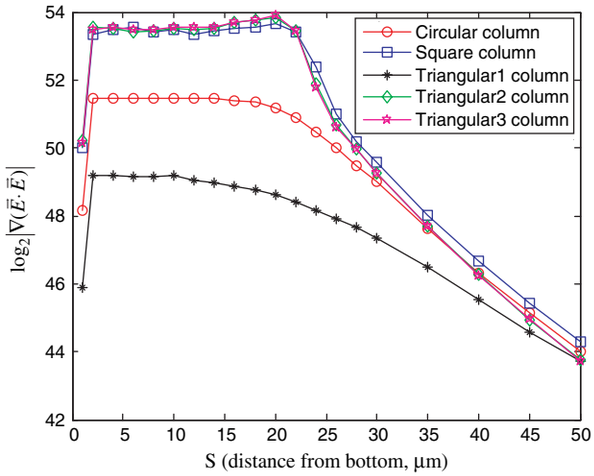

Fig. 3. The electric field intensity gradient as a function of the distance from channel floor for various electrode shapes.

The electric field intensity gradient is sampled at vertical planes, the distance from the channel floor is 10 μm, and the gradient magnitude is taken as a logarithm i.e., $\log_2|\nabla(E\cdot E)|$. The geometrical parameters are selected as $R = D = L = 20$ μm. The applied voltage of two diagonal electrodes is the same in which one is at 5 V_p and the other is grounded. It is observed that the gradient maxima in the electric field occurs near the electrode edges and varies from point to point for the same height as the gradient is proportional to the curvature of the point at the electrode edges. It is also found that the gradient always points out towards the edges of electrode from the center of four electrodes denoted by x and y components of the field gradient in the electric field intensity as shown in the arrowhead diagram Figure 5(a). Figure 5(b) presents the vertical or z component of the electric field intensity gradient for square column quadruple electrodes, where the arrow head direction and length represent local direction and magnitude of the gradient respectively. It also indicates that the field gradient always towards the channel floor. The

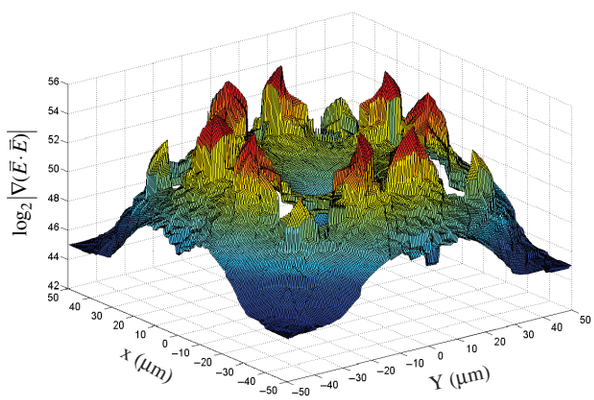

Fig. 4. The 3-D surface plots of field magnitude $\log_2|\nabla(E\cdot E)|$ of cross-section at the height of 10 μm above channel floor for a 20 μm height quadruple square column microelectrode array.

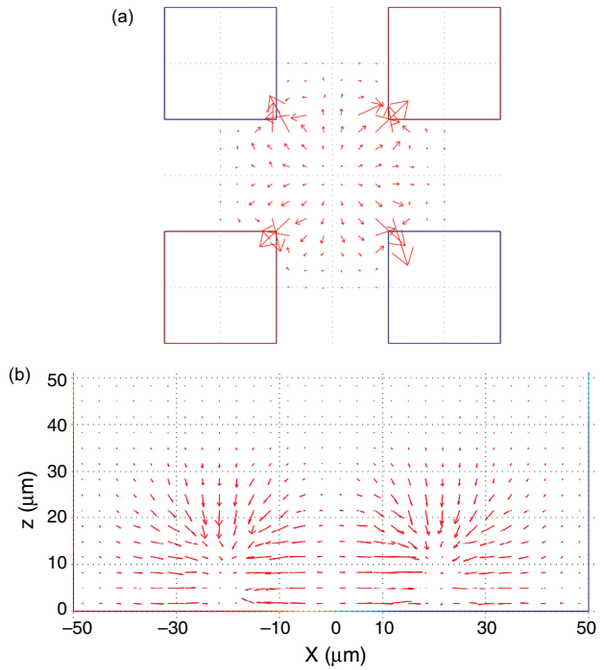

Fig. 5. (a) The gradient direction of electric field intensity, (b) The gradient magnitude in vertical plane at $y = 0$ for the 20 μm height square column quadruple microelectrode array.

plots show clearly the location of an isolated field minima, where in fact the field is zero at the center of the four electrodes, and the DEP force is also zero. Particles of a lower effective polarizability than that of surrounding suspending media will experience a negative DEP force and be directed towards the center point, which can be applied as a well-defined trapping well for nano-sized particle concentration, separation and focusing.[18]

3.3. Dependence on Electrode Voltage

Figure 6 plots the electric field intensity gradient as a function of applied voltage for various electrode geometric

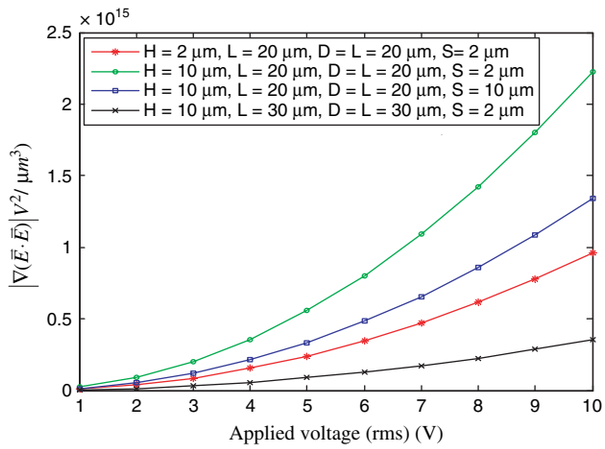

Fig. 6. The electric field intensity gradient as a function of applied voltage.

RESEARCH ARTICLE

parameters, such as H, L, D and S known as the electrode height, width, spacing and the distance of sampled points to the channel floor respectively. Over the range of voltages sampled, the data curves were fitted with a power law. For all voltages and electrode geometric parameters tested, the exponent derived as fitted data to reveal a squared magnitude dependence of the DEP force on the applied voltage ($|\nabla(\vec{E}\cdot\vec{E})| \propto V^2$) with a correlation coefficient of 1, which is consistent with the literature report.[20] Experimental work on voltage dependence has been demonstrated in literature, which showed similar conclusions with our predictions.[21]

3.4. Dependence on Electrode Width, Spacing and Height

Generally, as the edge-to-edge electrode spacing increases, the DEP force decreases. In Figure 7(a), four electrode height parameters are chosen and the gradient magnitude is calculated for various electrode widths when electrode spacing is equal to electrode width and the distance to

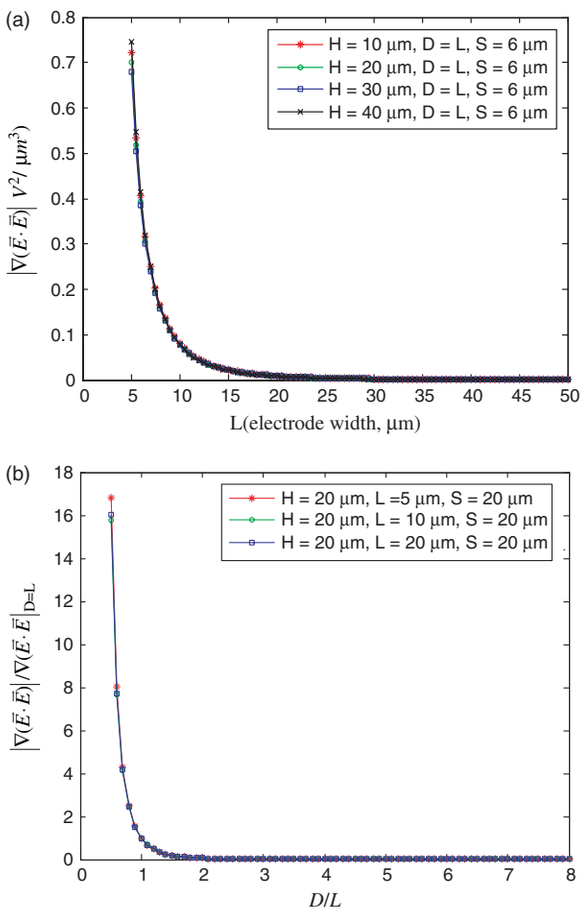

Fig. 7. (a) The electric field intensity gradient as a function of electrode width, (b) The normalized gradient magnitude as a function of spacing between electrodes.

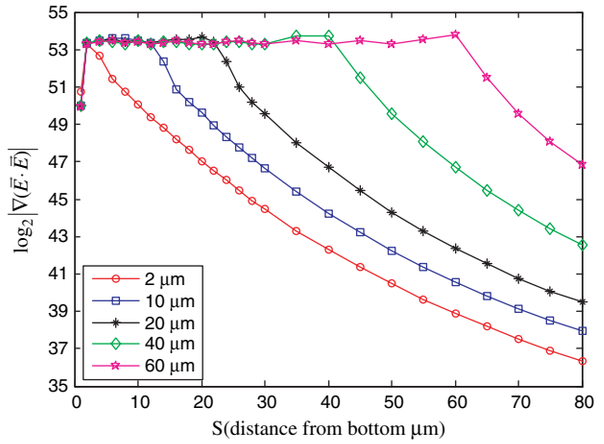

Fig. 8. The electric field intensity gradient as a function of distance from channel floor.

floor S kept at 6 μm. By fitted curve data, it is found that $|\nabla(\vec{E}\cdot\vec{E})| \propto L^{-3}$ for various electrode heights. By considering the effect of electrode spacing D, the gradient is normalized by ratio of the gradient at D/L over the gradient at $D = L$ as shown in Figure 7(b). It is observed that $|\nabla(\vec{E}\cdot\vec{E})|/|\nabla(\vec{E}\cdot\vec{E})|_{D=L} \propto (D/L)^{-4}$ for various lengths L such as 5 μm, 10 μm and 20 μm, and the gradient decreases exponentially as the spacing increases. These calculations are also in qualitative agreement with literature experimental reports.[21,22] Figure 8 illustrates the gradient plotted as a function of the distance from channel bottom for various electrode heights. It is concluded that the gradient almost keeps constant as the distance from the channel floor increases in case of the distance from channel floor is smaller than the height of electrode. Above that, the gradient decays rapidly as the distance from the channel floor increases, and similar conclusion is also presented in literature.[12] It is obvious that the effective DEP force extends much largely within fluid as the height of electrode increases. Therefore, a 3-D electrode design used for DEP manipulation is suitable significantly to improve the efficiency, flexibility and throughput through proper design of the electrode height and control of the manipulation region of nanoparticles inside fluid channel.[23]

4. CONCLUSIONS

We developed a basic design methodology for 3-D carbon microelectrode array configurations to optimize DEP manipulation of nanoparticles within fluids. The outcomes demonstrate that square electrode shape is more effective than circular or triangular electrode shapes, and electrode spacing, width, and height are critical design parameters for seeking optimal DEP manipulation. 3-D structure configurations will significantly improve the manipulation efficiency with high degree of precision, flexibility and

RESEARCH ARTICLE

throughput. The gradient magnitude increases exponentially as the electrode spacing and width is reduced, and the effective DEP force extends much largely within fluid as the height of electrode increases. Additionally, a squared magnitude dependence of the DEP force on the applied voltage is also observed. These findings will provide critical guidelines for optimal design of 3-D carbon microelectrode array and its integration with on-chip devices.

Acknowledgments: This research is sponsored by National Science Foundation of China (No. 50875103, 90923019) and Wuhan National Laboratory for Optoelectronics.

References and Notes

1. R. Krupke, F. Hennrich, H. V. Lohneysen, and M. M. Kappes, *Science* 301, 344 **(2003)**.
2. L. Zheng, J. P. Brody, and P. J. Burke, *Biosens. Bioelectron* 20, 606 **(2004)**.
3. T. Arun, J. Kadaksham, P. Singh, and N. Aubry, *Electrophoresis* 25, 3625 **(2004)**.
4. H. A. Pohl and I. Hawk, *Separation Science* 152, 647**(1996)**.
5. H. A. Pohl, Dielectrophoresis, The Behavior of Neutral Matter in Nonuniform Electric Fields, Cambridge University Press, Cambridge **(1978)**.
6. L. Cui and H. Morgan, *J. Micromech. Microeng.* 10, 72 **(2000)**.
7. T. P. Hunt, H. Lee, and R. M. Westervelta, *Appl. Phys. Lett.* 85, 6421 **(2004)**.
8. Y. Liu, K. Oh, J. G. Bai, and C. Chang, *Comput. Methods Appl. Mech. Energy* 197, 2156 **(2008)**.
9. S. Golan, D. Elata, and U. Dinnar, *Sens. Actuators, A* 142, 138 **(2008)**.
10. L. Yu, C. Iliescu, G. Xu, and F. E. H. Tay, *J. Microelectromech. Sys.* 15, 1120 **(2007)**.
11. C. Wang, G. Jia, L. H. Taherabadi, and M. J. Madou, *J. Microelecmech. Sys.* 14, 348 **(2005)**.
12. B. Y. Park and M. J. Madou, *Electrophoresis* 26, 3745 **(2005)**.
13. C. Iliescu, G. Xu, F. C. Loe, P. L. Ong, and F. E. H. Tay, *Electrophoresis* 28, 1107 **(2007)**.
14. N. G. Green, A. Ramos, and H. Morgan, *J. Phys. D: Appl. Phys.* 33, 632 **(2000)**.
15. O. D. Velev and K. H. Bhatt, *Soft Matter.* 2, 738 **(2006)**.
16. A. Subramanian, B. Vikramaditya, L. Dong, D. Bell, and B. J. Nelson, Robotics: Science and System, MIT Press, Cambridge, MA **(2005)**, Vol. 1.
17. C. Rosales, *Electrophoresis* 27, 1984 **(2006)**.
18. S. K. Thamida and H.-C. Chang, *Phys. Fluids* 14, 4315 **(2002)**.
19. I. F. Cheng and H. C. Chang, *Biomicrofluidics* 1, 021503 **(2007)**.
20. A. S. Bahaj and A. G. Bailey, *J. Phys. D: Appl. Phys.* 12, L109 **(1979)**.
21. D. S. Clague and E. K. Wheeler, *Phys. Rev. E* 64, 026605 **(2001)**.
22. J. Suehiuro and R. Pethig, *J. Phys. D: Appl. Phys.* 31, 3298 **(1998)**.
23. T. Muller, G. Gradl, S. Howtiz, S. Shiirley, Th. Schnelle, and G. Fuhr, *Biosens. Bioelectron.* 14, 247 **(1999)**.

Received: 30 December 2009. Revised/Accepted: 30 August 2010.

RESEARCH ARTICLE